Myocardial SPECT perfusion defect size compared to infarct size by delayed gadolinium-enhanced magnetic resonance imaging in patients with acute or chronic infarction.

Hedström, Erik; Palmer, John; Ugander, Martin; Arheden, Håkan

Published in:
Clinical Physiology and Functional Imaging

DOI:
10.1111/j.1475-097X.2004.00579.x

2004

Clin Physiol Funct Imaging (2004) **24,** pp380–386

Myocardial SPECT perfusion defect size compared to infarct size by delayed gadolinium-enhanced magnetic resonance imaging in patients with acute or chronic infarction

Erik Hedström[1], John Palmer[2], Martin Ugander[1] and Håkan Arheden[1]

Departments of [1]Clinical Physiology and [2]Medical Radiation Physics, Lund University Hospital, Lund, Sweden

Correspondence

Håkan Arheden, Associate Professor, Department of Clinical Physiology, Lund University Hospital, SE-221 85 Lund, Sweden
E-mail: hakan.arheden@klinfys.lu.se

Accepted for publication

Received 9 April 2004;
accepted 6 August 2004

Key words

magnetic resonance imaging; myocardial infarction; myocardial ischaemia; perfusion; scintigraphy; single photon emission computed tomography

Summary

Background: Single photon emission computed tomography (SPECT) perfusion imaging has been considered a reference method for non-invasive estimation of infarct size in man. Recently, delayed gadolinium-enhanced magnetic resonance imaging (DE-MRI) has evolved as an accurate tool to quantify infarct size. Therefore, the present study was designed to compare perfusion defect size by SPECT to hyperenhanced volume by DE-MRI.

Methods: DE-MRI was performed in 30 patients. Fourteen were patients with revascularized first-time acute infarctions, eight revascularized chronic infarctions, and eight clinically referred non-revascularized patients. SPECT was performed in the same patients and analysed by a commercial package.

Results: The hypoperfused volume by SPECT was larger than the hyperenhanced volume by DE-MRI by 8 ± 8 ml ($6\% \pm 5$ percentage points), 10 ± 18 ml ($6\% \pm 11$ percentage points), and 26 ± 30 ml ($12\% \pm 10$ percentage points) in the acute, chronic and clinical populations, respectively. Left ventricle wall volume was smaller by SPECT in all settings.

Conclusion: The SPECT perfusion defect size was comparable with but generally slightly larger than the hyperenhanced volume by DE-MRI in both absolute and relative terms in patients with acute and chronic infarction. The results may be related to systematic differences between modalities but could also be influenced by biological phenomena such as wall thinning or hypoperfused but viable myocardium.

Introduction

The size of irreversible injury following an acute myocardial infarction has been shown to influence function and remodelling of the left ventricle (LV) (Feild *et al.*, 1972; Warren *et al.*, 1988) and has also proved to be an important predictor of mortality (Braunwald, 1989; Miller *et al.*, 1995). Therapy, such as thrombolysis or percutaneous transluminal coronary angioplasty (PTCA) that leads to reperfusion, limits infarct size (Braunwald, 1987, 1989; Gibbons *et al.*, 1994). To verify successful treatment in the acute setting, a reliable method for assessing the presence, extent, and location of infarcted myocardium is therefore of clinical importance (Gibbons *et al.*, 2000; Lund *et al.*, 2001). This is also the case in chronic myocardial infarction when determining appropriate treatment and monitoring outcome. Several approaches in the clinical setting can be used to directly or indirectly monitor treatment and infarct size, such as ECG (Hinohora *et al.*, 1988), biochemical markers of injury (Licka *et al.*, 2002), echocardiography (Shen *et al.*, 1991), metabolic activity by positron emission tomography (PET) (Chareonthaitawee *et al.*, 2002), or relative distribution of perfusion by myocardial single photon emission computed tomography (SPECT) perfusion imaging (Gibbons *et al.*, 2000). Scintigraphy using ^{201}Tl- or ^{99m}Tc-labelled perfusion agents such as sestamibi and tetrofosmin has often been used as a reference method to estimate infarct size (Miller *et al.*, 1995; Gibbons *et al.*, 2000) and to monitor invasive therapy (van der Wall *et al.*, 1990; Behrenbeck *et al.*, 1991; Gibbons *et al.*, 2000). Delayed gadolinium-enhanced magnetic resonance imaging (DE-MRI) has emerged as a useful method to image myocardial infarction and has in animal studies been shown to correlate well to histologically determined infarct size using triphenyltetrazolium chloride (TTC) staining (Kim *et al.*, 1999; Fieno *et al.*, 2000). Comparison of SPECT and DE-MRI for detection of non-transmural infarcts has shown that SPECT and DE-MRI detect transmural infarcts at similar rates although

non-transmural infarcts detected by DE-MRI may be missed by SPECT (Wagner *et al.*, 2003).

Therefore, the present study was designed to compare perfusion defect size by SPECT to the hyperenhanced volume by DE-MRI, in revascularized acute and chronic myocardial infarction, as well as in a non-revascularized population with chronic infarction.

Methods

All study patients had undergone myocardial infarction based on standard criteria as listed in the ACC/AHA guidelines for the management of patients with ST-elevation myocardial infarction (http://www.acc.org/clinical/guidelines/stemi/). The acute and chronic populations were revascularized and therefore less likely to have hypoperfused but viable myocardium. The clinical population was chosen as a non-revascularized group.

Acute study population

Fourteen patients (13 men, mean age 61 years, range 42–78 years) with no earlier evidence of myocardial infarction, presenting with acute ischaemia due to an occluded coronary artery, were included prospectively in the study. They underwent primary PTCA resulting in TIMI 3 flow in the opened artery. All patients received GPIIb/IIIa inhibitor during PTCA and were transferred to the coronary care unit for conventional therapy.

Chronic study population

Eight patients (eight men, mean age 65 years, range 57–76 years) with LV ejection fraction of <50% by echocardiography who underwent first-time elective coronary artery bypass grafting (CABG) without simultaneous valve repair were included prospectively.

Clinical study population

Eight clinically referred patients (seven men, mean age 68 years, range 57–74 years) who had undergone SPECT perfusion imaging were included and scheduled for DE-MRI.

Study protocol

The protocol and procedures were approved by the research ethics committee at Lund University Hospital, Sweden. Subjects were included after written informed consent. SPECT and DE-MRI were performed to determine the perfusion defect size and hyperenhanced volume, respectively.

The MRI was performed 6–9 days (median 7·5) after PTCA, and 28–38 days (median 32·5) after CABG in the acute and chronic population, respectively. SPECT was performed 0–5 days (median 0) and 0–1 day (median 0) after MRI in the acute and chronic population, respectively. MRI of the clinical population was performed 0–63 days (median 3·5) after SPECT. All patients were considered to be adequately medicated and were free from chest pain at time of imaging. The size of the perfusion defect measured by SPECT was compared with the hyperenhanced volume measured by DE-MRI.

SPECT imaging

Depending on body weight, 500–700 MBq ^{99m}Tc-labelled tetrofosmin (Amersham Health, Buckinghamshire, UK) was injected at least 30 min before SPECT. The acquisition was performed within 3 h from isotope injection according to the standard clinical protocol at rest using a dual-head camera (ADAC, Milpitas, CA, USA). The subject was placed in supine position and imaged in steps of 5·6 degrees using a 64 × 64 matrix with a pixel size of 5·02 mm. Image acquisition time was approximately 25 min.

SPECT image analysis

Short- and long-axis images gated to ECG were reconstructed, covering the LV (Fig. 1a). This was done using a commercial application (AutoSPECT+Instill^{TM} 6·0, ADAC) with an iterative method (maximum-likelihood expectation-maximization), using 12 iterations and a Butterworth filter with a cut-off value of 0·6 and an order of 5·0. Analysis of SPECT perfusion size is subject to a variety of technical and interpretation issues (Kojima *et al.*, 1989; King *et al.*, 1991; Ceriani *et al.*, 1996; Eisner & Patterson, 1999). We therefore chose to evaluate SPECT data by a validated (Germano *et al.*, 2000; Sharir *et al.*, 2000) and widely used commercial package (AutoQUANT^{TM} 4.3.1 and a standard database; ADAC), in line with clinical practice, rather than to elaborate on the analysis details. LV wall volume (LVWV) and perfusion defect size were quantified in millilitre.

Magnetic resonance imaging

Either a 1·5 T system (Magnetom Vision, Siemens, Erlangen, Germany) with a CP body array coil or a 1·5 T system (Philips Intera CV, Philips, Best, the Netherlands) with a cardiac synergy coil was used. The subject was placed in supine position. Short- and long-axis images were acquired, covering the LV. The gradient-recalled echo (GRE) cine sequence and the segmented inversion-recovery (IR) GRE sequence were triggered by ECG and images were acquired during breath hold of approximately 15 s. The short-axis GRE cine images (slice thickness 8 mm, slice gap 2 mm) were used to measure the volume of the LV wall. The delayed gadolinium-enhanced IR-GRE images (slice thickness 8 mm, slice gap 2 mm) were used to measure the hyperenhanced volume. DE-MRI using the IR-GRE sequence utilizes an increase in regional fractional distribution of extracellular MRI contrast media within the injured area (Tong *et al.*, 1993; Saeed *et al.*, 1994; Arheden *et al.*, 1999; Flacke *et al.*, 2001) to achieve contrast between viable and non-viable

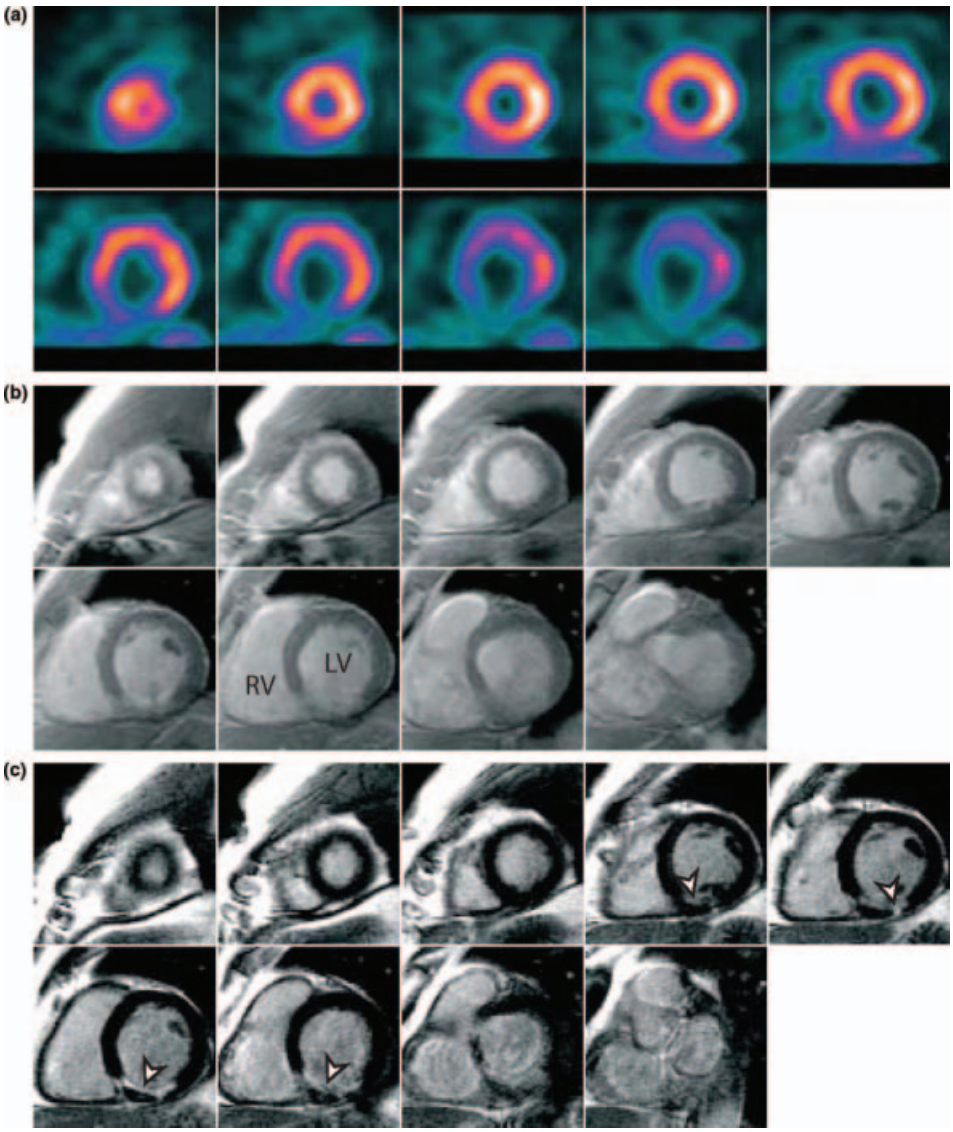

Figure 1 Images from a patient with an acute infarction in the inferior wall, showing short axis slices from apex to base by (a) SPECT. Corresponding images by (b) cine MRI, and (c) DE-MRI. Arrowheads indicate infarcted area (white). LV, left ventricle; RV, right ventricle.

myocardium (Simonetti *et al.*, 2001). A commercially available gadolinium-based contrast agent (acute and clinical populations: gadoteric acid, Gd-DOTA, Guerbet, Gothia Medical AB, Billdal, Sweden; chronic and clinical populations: gadopentetate dimeglumine, Gd-DTPA, Schering Nordiska AB, Järfälla, Sweden) was administered at a dose of 0·2 mmol per kilogram of body weight, and delayed gadolinium-enhanced images were acquired in the same views as those used for the GRE cine protocol. Images were acquired during end diastole 26 ± 8 (SD) min after gadolinium administration. The inversion time (TI) was adjusted to give null signal from the myocardium, typically giving a TI of 170 ms (range 150–210) or 270 ms (range 260–280) for the Siemens or Philips system, respectively, because of different imaging sequence construction between systems. Image acquisition time was approximately 40 min.

MR image analysis

Analysis of MR images was performed blinded to other results and patient information. All data were analysed using the program ImageJ ver 1·29x (http://rsb.info.nih.gov/ij/). In order to estimate interobserver variability, a subset of six patients was analysed by two observers. LVWV and hyperenhanced volumes were determined in end-diastolic (ED) images. Endocardial and epicardial borders were outlined manually on each ED and end-systolic frame in each short axis stack (Fig. 1b). Papillary muscles were included as LVWV. In the base of the LV where the left atrium was seen, only the portion of the slice that could be identified as LV was included. Hyperenhanced volume was outlined on the delayed contrast enhanced IR-GRE images throughout the LV (Fig. 1c). The long-axis images were used to verify the distribution of the hyperenhanced region. Total

myocardial and hyperenhanced volume were calculated as the planimetric measurements of each slice multiplied by slice thickness and slice gap. Relative hyperenhanced volume was expressed as percentage of the MRI LVWV.

Statistical analysis

Values were expressed as mean ± SD. Bland–Altman plots (Bland & Altman, 1986) were used to show differences between SPECT and MRI. A Wilcoxon signed-rank test was performed and $P<0{\cdot}05$ was considered to show significant difference.

Results

Acute study population

Hyperenhanced volume by DE-MRI ranged from 0 to 100 ml involving up to 39% of the LVWV. LVWV was smaller by SPECT compared with MRI (23 ± 22 ml; $P = 0{\cdot}001$; Fig. 2a). The hypoperfused volume by SPECT was in absolute and relative terms larger than the hyperenhanced volume by DE-MRI (8 ± 8 ml; $P = 0{\cdot}002$; Fig. 2b; 6% ± 5 percentage points; $P = 0{\cdot}001$; Fig. 2c).

Chronic study population

Hyperenhanced volume by DE-MRI ranged from 3 to 40 ml involving up to 17% of the LVWV. LVWV was smaller by SPECT compared with MRI (36 ± 26 ml; $P = 0{\cdot}016$; Fig. 2a). The hypoperfused volume by SPECT was in absolute and relative terms larger than the hyperenhanced volume by DE-MRI (10 ± 18 ml; $P = 0{\cdot}344$; Fig. 2b; 6% ± 11 percentage points; $P = 0{\cdot}344$; Fig. 2c).

Clinical study population

Hyperenhanced volume by DE-MRI ranged from 14 to 53 ml involving up to 29% of the LVWV. Mean LVWV did not differ between SPECT and MRI (0 ± 46 ml; $P = 0{\cdot}438$; Fig. 2a). The hypoperfused volume by SPECT was in absolute and relative terms larger than the hyperenhanced volume by DE-MRI (26 ± 30 ml; $P = 0{\cdot}047$; Fig. 2b; 12% ± 10 percentage points; $P = 0{\cdot}023$; Fig. 2c).

Interobserver variability

In the present MRI material interobserver variability was found to be 1 ± 4 ml (0 ± 3%) for LVWV and 0 ± 1 ml (1 ± 3%) for infarct size.

Discussion

The results show that the hypoperfused volume by myocardial SPECT perfusion imaging was generally slightly larger than the hyperenhanced volume by delayed contrast enhanced MRI. In addition, LVWV by SPECT was smaller compared with MRI in man in both the acute and chronic setting.

The results of the present study in patients are consistent with previous results comparing SPECT and explanted hearts showing that the relative hypoperfused volume measured by *ex vivo* SPECT is slightly larger than *ex vivo* measurements of relative infarct size by TTC (Medrano *et al.*, 1996). SPECT has also been shown to underestimate the amount of viable myocardium when compared with PET (Arrighi *et al.*, 1997). As SPECT depicts a perfusion defect, it is possible that not only the infarcted area but also a border zone of hypoperfused but viable myocardium is included. This border zone, previously described experimentally (Reimer *et al.*, 1977), may explain the discrepancy between perfusion defect size and hyperenhanced volume by DE-MRI. In the chronic as well as in the clinical study population, the perfusion defect may reflect hypoperfused but viable, so called hibernating myocardium (Braunwald & Rutherford, 1986) whereby a larger perfusion defect size may be measured compared with hyperenhanced volume by DE-MRI. In addition, wall thinning by itself, in absence as well as in presence of infarction, may be detected as a perfusion defect by SPECT (Smith *et al.*, 1997; Eisner & Patterson, 1999), giving rise to a larger perfusion defect size compared with hyperenhanced volume by DE-MRI. In the acute study population, no thinning but however stunning (Braunwald & Kloner, 1982; Kloner *et al.*, 2001) and thereby normally perfused but hypofunctioning myocardium may be present which possibly may be depicted as a perfusion defect because of absence of thickening-related count increase. Furthermore, systematic differences between SPECT and MRI may depend on technical issues such as temporal and spatial resolution.

In cases where the perfusion defect size by SPECT was smaller than the hyperenhanced volume by DE-MRI (Fig. 2b), this could for example be because of the presence of non-transmural infarctions with otherwise well perfused epicardial regions, resulting in possible underdetection and underestimation of the hypoperfused volume by SPECT (Elkamhawy & Chandna, 2001; Wagner *et al.*, 2003). However, in the current study not only non-transmural but also transmural infarctions were in some cases found smaller by SPECT compared with DE-MRI.

It has been proposed that the accuracy of the algorithms used for determination of the SPECT perfusion defect size may depend on myocardial wall thickness which may be of specific importance in cases of larger perfusion defects giving rise to inconsistencies in perfusion defect detection (Eisner & Patterson, 1999).

A smaller LVWV by SPECT than by MRI is likely because of an underestimation on behalf of SPECT rather than overestimation by MRI, since previous findings show that MRI of the LVWV correlates well with autopsy findings (Caputo *et al.*, 1987; Lund *et al.*, 2000).

Limitations of the study

Patients in the clinical population who have not undergone revascularization treatment may have hypoperfused but viable

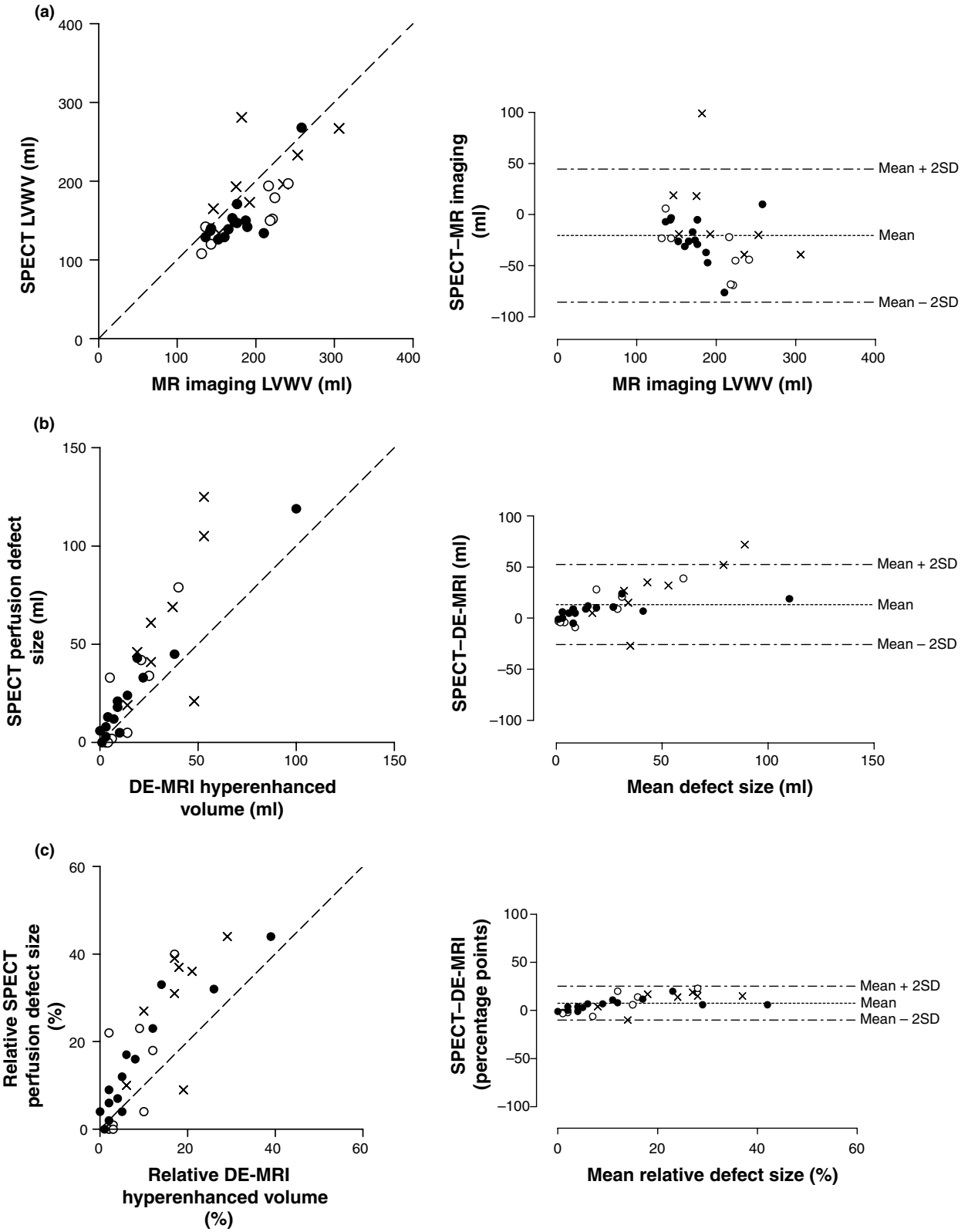

Figure 2 (a) Agreement (left) of LVWV between SPECT and MRI in the acute (●), chronic (○), and clinical (×) populations. Bland–Altman plot (right) showing differences between SPECT and MRI. (b) Corresponding data and analysis for perfusion defect size by SPECT and hyperenhanced volume by DE-MRI. (c) Corresponding data and analysis for relative perfusion defect by SPECT and relative hyperenhanced volume by DE-MRI. LVWV, left ventricle wall volume. Dashed line indicates line of equality.

myocardium present, so called hibernating myocardium. This may give rise to a much larger perfusion defect size by SPECT compared with hyperenhanced volume by DE-MRI. However, to address this issue, we studied revascularized patients in the acute and chronic populations.

Conclusion

The present study has shown a better agreement between SPECT and DE-MRI to estimate infarct size in revascularized myocardial infarction compared with non-revascularized infarction. The perfusion defect size by SPECT is generally slightly larger than the hyperenhanced volume by DE-MRI in both absolute and relative terms. The results are likely related to systematic differences between modalities but could also be influenced by biological phenomena such as wall thinning or hypoperfused but viable myocardium.

Acknowledgments

The authors would like to express their gratitude to Ann-Helen Arvidsson, technician, for help with reconstruction of the SPECT images. This work was supported by grants from the Swedish Research Council, Swedish Heart Lung Foundation, Lund University Faculty of Medicine, and Region of Scania.

References

Arheden H, Saeed M, Higgins CB, Gao DW, Bremerich J, Wyttenbach R, Dae MW, Wendland MF. Measurement of the distribution volume of gadopentetate dimeglumine at echo-planar MR imaging to quantify myocardial infarction: comparison with 99mTc-DTPA autoradiography in rats. *Radiology* (1999); **211**: 698–708.

Arrighi JA, Ng CK, Dey HM, Wackers FJ, Soufer R. Effect of left ventricular function on the assessment of myocardial viability by technectium-99m sestamibi and correlation with positron emission tomography in patients with healed myocardial infarcts or stable angina pectoris, or both. *Am J Cardiol* (1997); **80**: 1007–1013.

Behrenbeck T, Pellikka PA, Huber KC, Bresnahan JF, Gersh BJ, Gibbons RJ. Primary angioplasty in myocardial infarction: assessment of improved myocardial perfusion with technetium-99m isonitrile. *J Am Coll Cardiol* (1991); **17**: 365–372.

Bland JM, Altman DG. Statistical methods for assessing agreement between two methods of clinical measurement. *Lancet* (1986); **1**: 307–310.

Braunwald E. The path to myocardial salvage by thrombolytic therapy. *Circulation* (1987); **76**: II2–II7.

Braunwald E. Myocardial reperfusion, limitation of infarct size, reduction of left ventricular dysfunction, and improved survival. Should the paradigm be expanded? *Circulation* (1989); **79**: 441–444.

Braunwald E, Kloner RA. The stunned myocardium: prolonged, postischemic ventricular dysfunction. *Circulation* (1982); **66**: 1146–1149.

Braunwald E, Rutherford JD. Reversible ischemic left ventricular dysfunction: evidence for the ''hibernating myocardium''. *J Am Coll Cardiol* (1986); **8**: 1467–1470.

Caputo GR, Tscholakoff D, Sechtem U, Higgins CB. Measurement of canine left ventricular mass by using MR imaging. *AJR Am J Roentgenol* (1987); **148**: 33–38.

Ceriani L, Verna E, Giovanella L, Bianchi L, Roncari G, Tarolo GL. Assessment of myocardial area at risk by technetium-99m sestamibi during coronary artery occlusion: comparison between three tomographic methods of quantification. *Eur J Nucl Med* (1996); **23**: 31–39.

Chareonthaitawee P, Schaefers K, Baker CS, Turkheimer F, Stegger L, Banner NR, Yacoub M, Bonser RS, Iozzo P, Camici PG, Rimoldi O. Assessment of infarct size by positron emission tomography and [18F]2-fluoro-2-deoxy-D-glucose: a new absolute threshold technique. *Eur J Nucl Med Mol Imaging* (2002); **29**: 203–215.

Eisner RL, Patterson RE. The challenge of quantifying defect size and severity: reality versus algorithm. *J Nucl Cardiol* (1999); **6**: 362–371.

Elkamhawy AA, Chandna H. Minimum detectable defect thickness in SPECT myocardial perfusion test: phantom study with (99m)Tc and (201)Tl. *J Nucl Med Technol* (2001); **29**: 183–188.

Feild BJ, Russell RO, Jr, Dowling JT, Rackley CE. Regional left ventricular performance in the year following myocardial infarction. *Circulation* (1972); **46**: 679–689.

Fieno DS, Kim RJ, Chen EL, Lomasney JW, Klocke FJ, Judd RM. Contrast-enhanced magnetic resonance imaging of myocardium at risk: distinction between reversible and irreversible injury throughout infarct healing. *J Am Coll Cardiol* (2000); **36**: 1985–1991.

Flacke SJ, Fischer SE, Lorenz CH. Measurement of the gadopentetate dimeglumine partition coefficient in human myocardium in vivo: normal distribution and elevation in acute and chronic infarction. *Radiology* (2001); **218**: 703–710.

Germano G, Kavanagh PB, Waechter P, Areeda J, Van Kriekinge S, Sharir T, Lewin HC, Berman DS. A new algorithm for the quantitation of myocardial perfusion SPECT. I: technical principles and reproducibility. *J Nucl Med* (2000); **41**: 712–719.

Gibbons RJ, Christian TF, Hopfenspirger M, Hodge DO, Bailey KR. Myocardium at risk and infarct size after thrombolytic therapy for acute myocardial infarction: implications for the design of randomized trials of acute intervention. *J Am Coll Cardiol* (1994); **24**: 616–623.

Gibbons RJ, Miller TD, Christian TF. Infarct size measured by single photon emission computed tomographic imaging with (99m)Tc-sestamibi: a measure of the efficacy of therapy in acute myocardial infarction. *Circulation* (2000); **101**: 101–108.

Hinohora T, Wagner NB, Cobb FR, Coleman RE, Pope JE, Haisty WK, Wagner GS. An ischemic index from the electrocardiogram to select patients with low left ventricular ejection fraction for coronary artery bypass grafting. *Am J Cardiol* (1988); **61**: 288–291.

Kim RJ, Fieno DS, Parrish TB, Harris K, Chen EL, Simonetti O, Bundy J, Finn JP, Klocke FJ, Judd RM. Relationship of MRI delayed contrast enhancement to irreversible injury, infarct age, and contractile function. *Circulation* (1999); **100**: 1992–2002.

King MA, Long DT, Brill AB. SPECT volume quantitation: influence of spatial resolution, source size and shape, and voxel size. *Med Phys* (1991); **18**: 1016–1024.

Kloner RA, Arimie RB, Kay GL, Cannom D, Matthews R, Bhandari A, Shook T, Pollick C, Burstein S. Evidence for stunned myocardium in humans: a 2001 update. *Coron Artery Dis* (2001); **12**: 349–356.

Kojima A, Matsumoto M, Takahashi M, Hirota Y, Yoshida H. Effect of spatial resolution on SPECT quantification values. *J Nucl Med* (1989); **30**: 508–514.

Licka M, Zimmermann R, Zehelein J, Dengler TJ, Katus HA, Kubler W. Troponin T concentrations 72 hours after myocardial infarction as a serological estimate of infarct size. *Heart* (2002); **87**: 520–524.

Lund GK, Wendland MF, Shimakawa A, Arheden H, Stahlberg F, Higgins CB, Saeed M. Coronary sinus flow measurement by means of velocity-encoded cine MR imaging: validation by using flow probes in dogs. *Radiology* (2000); **217**: 487–493.

Lund GK, Higgins CB, Wendland MF, Watzinger N, Weinmann HJ, Saeed M. Assessment of nicorandil therapy in ischemic myocardial injury by using contrast-enhanced and functional MR imaging. *Radiology* (2001); **221**: 676–682.

Medrano R, Lowry RW, Young JB, Weilbaecher DG, Michael LH, Afridi I, He ZX, Mahmarian JJ, Verani MS. Assessment of myocardial viability with 99mTc sestamibi in patients undergoing cardiac transplantation. A scintigraphic/pathological study. *Circulation* (1996); **94**: 1010–1017.

Miller TD, Christian TF, Hopfenspirger MR, Hodge DO, Gersh BJ, Gibbons RJ. Infarct size after acute myocardial infarction measured by quantitative tomographic 99mTc sestamibi imaging predicts subsequent mortality. *Circulation* (1995); **92**: 334–341.

Reimer KA, Lowe JE, Rasmussen MM, Jennings RB. The wavefront phenomenon of ischemic cell death. 1. Myocardial infarct size vs duration of coronary occlusion in dogs. *Circulation* (1977); **56**: 786–794.

Saeed M, Wendland MF, Masui T, Higgins CB. Reperfused myocardial infarctions on T1- and susceptibility-enhanced MRI: evidence for loss of compartmentalization of contrast media. *Magn Reson Med* (1994); **31**: 31–39.

Sharir T, Germano G, Waechter PB, Kavanagh PB, Areeda JS, Gerlach J, Kang X, Lewin HC, Berman DS. A new algorithm for the quantitation of myocardial perfusion SPECT. II: validation and diagnostic yield. *J Nucl Med* (2000); **41**: 720–727.

Shen WK, Khandheria BK, Edwards WD, Oh JK, Miller FA Jr, Naessens JM, Tajik AJ. Value and limitations of two-dimensional echocardiography in predicting myocardial infarct size. *Am J Cardiol* (1991); **68**: 1143–1149.

Simonetti OP, Kim RJ, Fieno DS, Hillenbrand HB, Wu E, Bundy JM, Finn JP, Judd RM. An improved MR imaging technique for the visualization of myocardial infarction. *Radiology* (2001); **218**: 215–223.

Smith WH, Kastner RJ, Calnon DA, Segalla D, Beller GA, Watson DD. Quantitative gated single photon emission computed tomography imaging: a counts-based method for display and measurement of regional and global ventricular systolic function. *J Nucl Cardiol* (1997); **4**: 451–463.

Tong CY, Prato FS, Wisenberg G, Lee TY, Carroll E, Sandler D, Wills J, Drost D. Measurement of the extraction efficiency and distribution volume for Gd-DTPA in normal and diseased canine myocardium. *Magn Reson Med* (1993); **30**: 337–346.

Wagner A, Mahrholdt H, Holly TA, Elliott MD, Regenfus M, Parker M, Klocke FJ, Bonow RO, Kim RJ, Judd RM. Contrast-enhanced MRI and routine single photon emission computed tomography (SPECT) perfusion imaging for detection of subendocardial myocardial infarcts: an imaging study. *Lancet* (2003); **361**: 374–379.

van der Wall EE, Niemeyer MG, de Roos A, Bruschke AV, Pauwels EK. Infarct sizing by scintigraphic techniques and nuclear magnetic resonance imaging. *Eur J Nucl Med* (1990); **17**: 83–90.

Warren SE, Royal HD, Markis JE, Grossman W, McKay RG. Time course of left ventricular dilation after myocardial infarction: influence of infarct-related artery and success of coronary thrombolysis. *J Am Coll Cardiol* (1988); **11**: 12–19.